RADIATION-MAGNETO-HYDRODYNAMICS MODELS FOR STAR FORMATION AND SYNTHETIC OBSERVATIONS

Commerçon B.[1], Levrier F.[1], Maury A. J.[2], Henning Th.[3], Launhardt R.[3] & Dullemond C.[4]

(1) LRA/LERMA Observatoire de Paris, (2) CfA Harvard-Smithsonian, (3) MPIA Heidelberg, (4) ZAH/ITA Heidelberg

Abstract

Although predicted by theoretical models, the existence of first hydrostatic cores (FHSC) has yet to be convincingly demonstrated by (sub)millimeter observations, and the multiplicity at this early stage of the star formation process is poorly constrained.

We present a possible identification strategy for FHSC candidates [1] and make predictions of ALMA dust continuum emission maps from these objects [2]. This is done by post-processing three state-of-the-art radiation-magneto-hydrodynamic (RMHD) 3D adaptive mesh refinement calculations of first hydrostatic core models performed with the RAMSES code. We compute the dust thermal continuum emission with the 3D radiative transfer code RADMC-3D. We compute spectral energy distributions (SED) and usual evolutionary stage indicators such as bolometric luminosity and temperature, and then produce synthetic ALMA observations using the simulator included in the GILDAS software package.

We show that under certain conditions, FHSCs can be identified from dust continuum emission at 24 μm and 70 μm. We also show that single SEDs cannot help in distinguishing between the formation scenarios of the FHSC, i.e., between the magnetized and non-magnetized models. We identify which combinations of the different ALMA bands and array configurations represent our best chance of solving the fragmentation issue in these objects. We thus demonstrate how ALMA will help in identifying the physical processes occurring within collapsing dense cores: If the magnetic field is playing a role, the emission pattern will show evidence of a pseudo-disk and even of a magnetically driven outflow, which pure hydrodynamical calculations cannot reproduce.

Initial setup

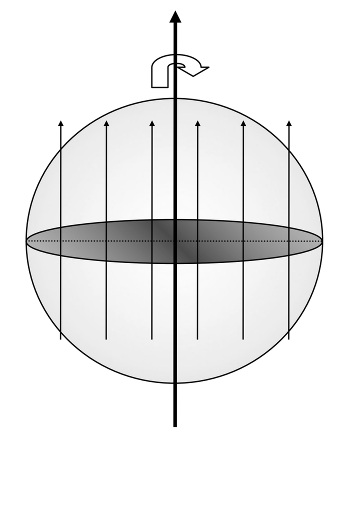

- 1 $M_\odot$ isolated dense core in solid body rotation
- uniform density & temperature
- *m*=2 azimuthal density perturbation
- magnetic field aligned with rotation axis
- **Resolution**: 10 pts/Jeans length (2 AU min)
- $\alpha = 0.35$ (E_{th}/E_{grav}), $\beta = 0.045$ (E_{rot}/E_{grav})
- $\mu = (M/\Phi)/(M/\Phi)_{crit}$

Opacity table from Semenov et al. (2003) for low temperature.

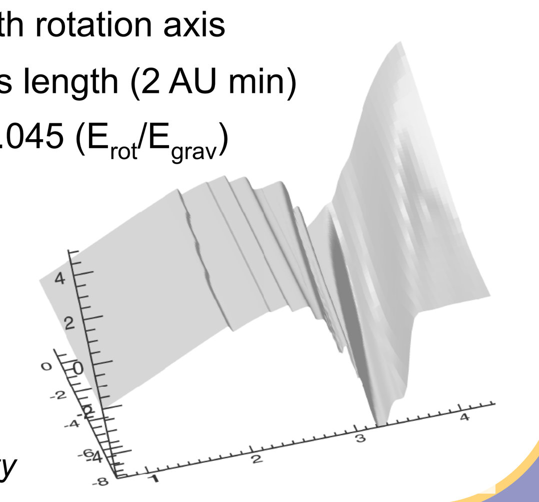

Rosseland mean opacity

TOOLS

Radiation-magneto-hydrodynamics

- Adaptive Mesh Refinement code RAMSES [3]
- **ideal MHD** approximation for **magnetic fields** [4,5]
- **grey FLD** approximation for **radiative transfer** [6]
- **no** H_2 dissociation
- mean Rosseland & Planck opacities from [7]

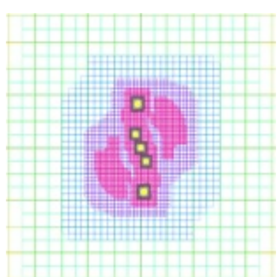

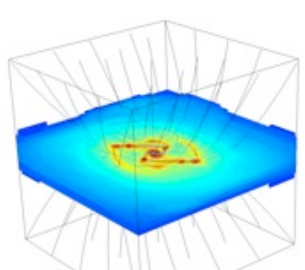

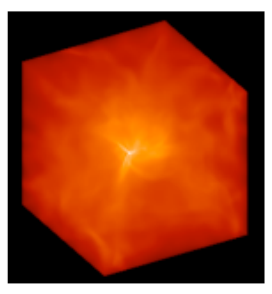

3D radiative transfer

We use the 3D RADMC-3D code (*Dullemond*, ITA-Heidelberg, Germany) to postprocess the RAMSES calculations.

★RADMC-3D features used:
- dust continuum emission
- line emission

★RADMC-3D outputs:
- dust emission maps
- spectral energy distribution
- line emission maps/profiles

Telescope simulator

We use the IRAM GILDAS simulator [11,12] to convolve to ALMA angular resolution.

RMHD results

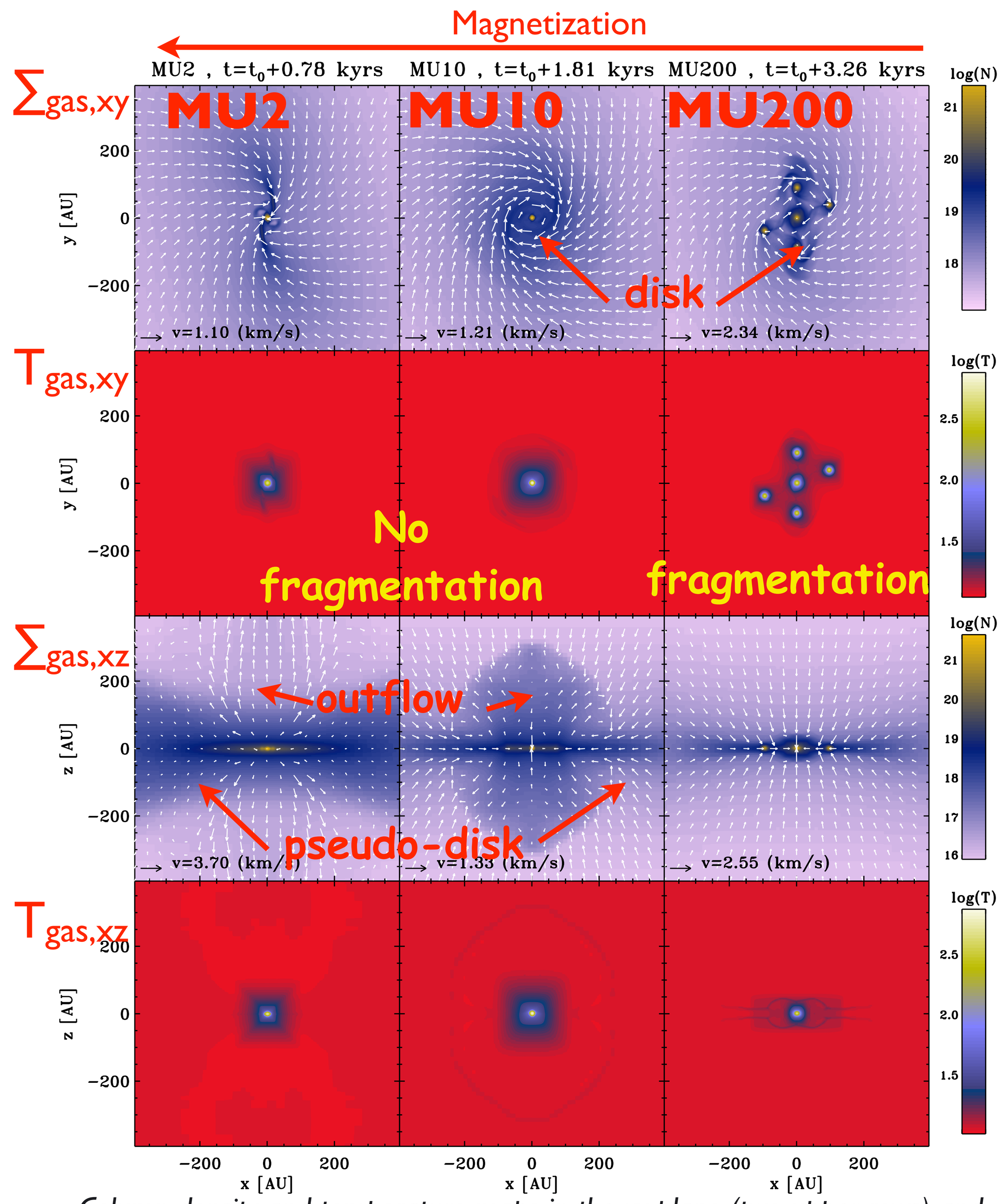

Column density and temperature maps in the xy-plane (two upper rows) and xz-plane (two lower rows) for the three RMHD calculations: MU2 (left), MU10 (middle), and MU200 (right). Scales are logarithmic, and column density N is given in cm^{-2}. Figure taken from [1].

The three models are representative of the wide variety of early evolutionary morphology, e.g., the formation of a disk or a pseudo-disk, outflow launching, and fragmentation.

FHSC lifetimes (kyr)

MU2	1.2
MU10	3
MU200	> 4

FHSC core lifetime depends on the magnetization level (the stronger B, the shorter lifetime). Strong magnetic fields induce strong magnetic braking and thus larger accretion rates [8].

Simulated ALMA dust emission observations

We predict what may be observed by ALMA when targeting FHSC candidates. To this end, we produce dust emission maps with RADMC-3D in bands 3, 4, 6, 7 and 9, and used these as input brightness distributions for the ALMA GILDAS simulator. We consider four typical configurations of the full array, but do not include the ALMA Compact Array (ACA).

To distinguish between the MU2 and MU200 models, it is necessary to resolve the fragmentation scale of a few AU. Of the four configurations considered here, C=15 and C=20 provide the best sampling of these spatial scales.

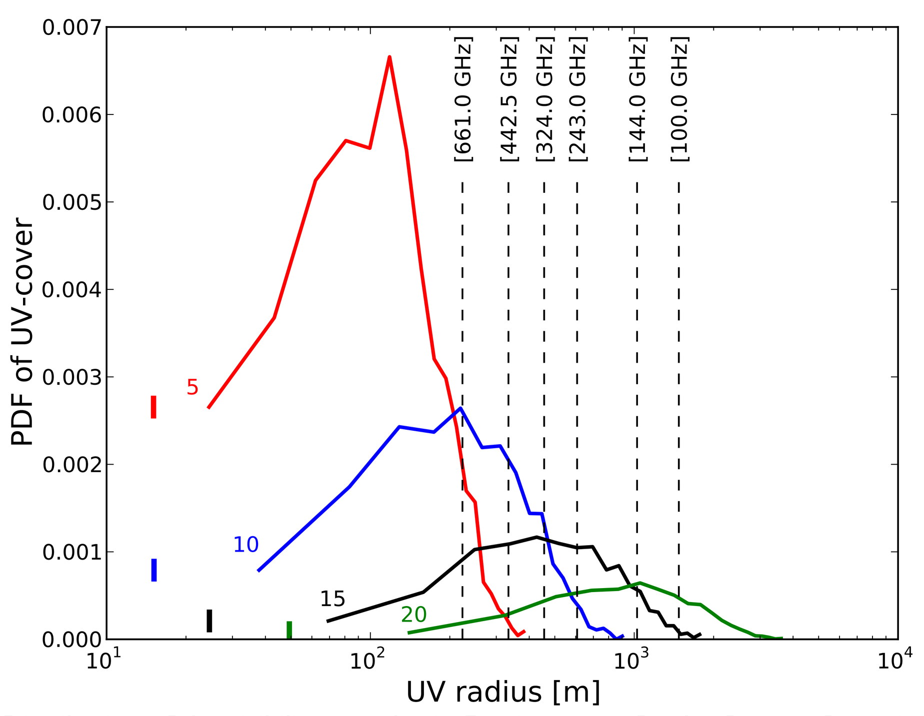

Distribution of the visibility samples in Fourier space for the four configurations of the array. The small vertical lines indicate the minimum baseline for each configuration, and the dashed lines indicate, for each frequency, the characteristic baselines corresponding to a physical scale of 10 AU, comparable to the fragmentation scale. Figure taken from [2].

Simulated emission maps show a clear distinction between the magnetized models (MU2 and MU10) and the quasi-hydro case MU200, and the different features from the RMHD models (disk, pseudo-disk, outflow) appear quite clearly and above the noise level in the simulated dust emission maps. The simulated maps presented here assume 18 minute runs of observation, so that many FHSC candidates may be observed in a single observing proposal.

Extended configurations have a large central hole in Fourier space, which means that they miss more of the large-scale flux than C=5 and C=10. This flux loss becomes more important at higher frequencies, because a given baseline then corresponds to smaller scales in the observed brightness distribution.

Overall, it appears that, for FHSC candidates at 150 pc, observing below 150 GHz with a configuration providing best sampling around 500 m to 1 km baselines provides a limited flux loss and the ability to resolve the fragmentation scale, thus suggesting an observing strategy for forthcoming ALMA proposals.

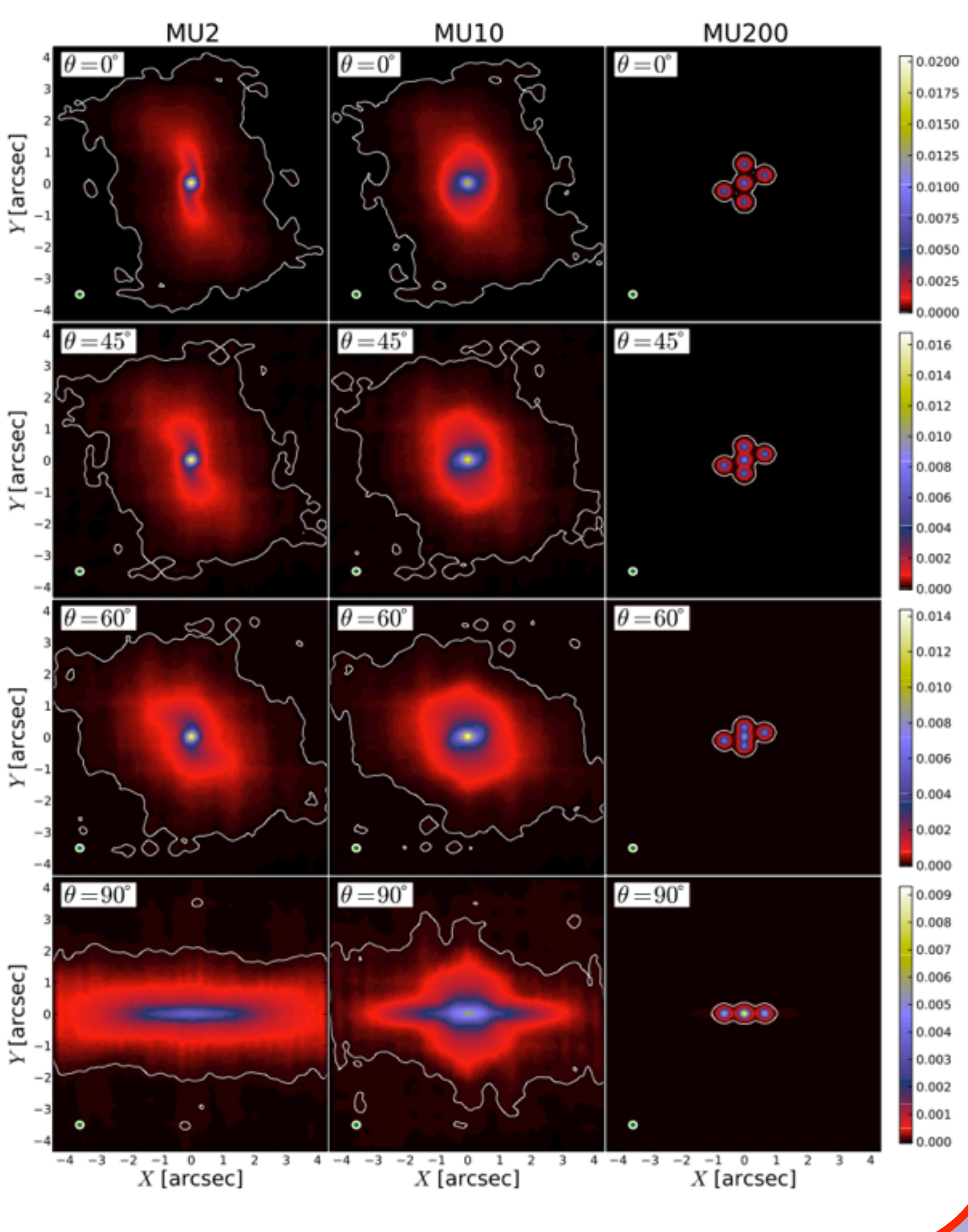

Simulated ALMA dust emission maps at 144 GHz in configuration C=20 for the MU2 (left), MU10 (middle) and MU200 (right) models. Four inclination angles are presented, from pole-on view (top) to edge-on view (bottom). Color scales are in Jy/beam and con- tours show the 3σ sensitivity limit in this band, with σ=16.05 μJy. The synthesized beam is shown in the bottom left corner of each plot. Figure taken from [2].

FHSC hunting with SED

★ **Spectral energy distribution: tool** to select first core candidates, to distinguish starless cores and first cores and to support observation proposals.

★ **Evolutionary sequence** in the SEDs and in color-color diagrams [1].

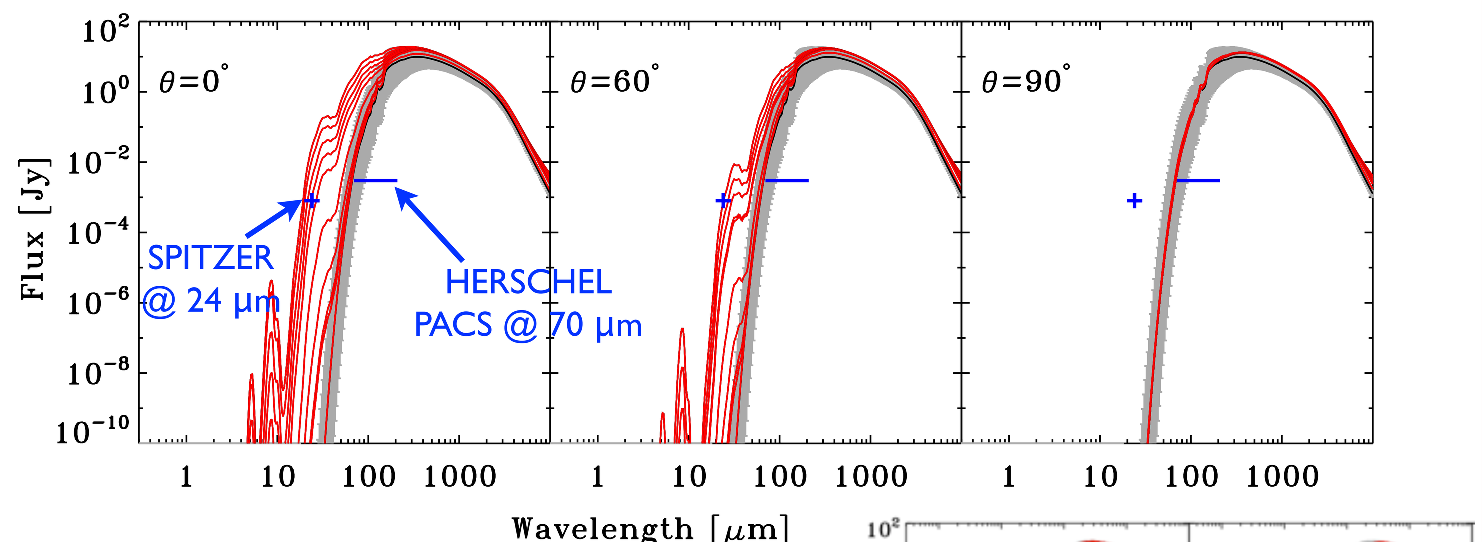

SED evolution as a function of time and inclination for the MU2 and MU200 models. The black line represents the SED when the FHSC has not yet been formed, whereas the red lines indicate SEDs after FHSC formation. The blue cross represents the sensitivity at 24 μm [9] and the horizontal blue line the sensitivity of the Herschel PACS instrument [10]. Figure taken from [1].

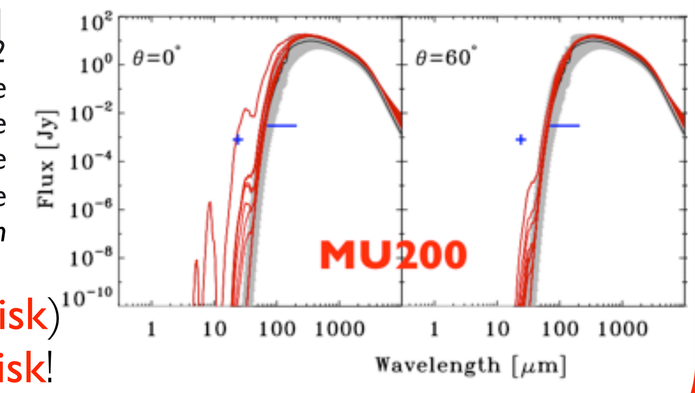

Similar SEDs in the MU2 model (no disk) and in the MU200 model, i.e. with a disk!

=> Issues in SED-fitting models for early Class 0?

CONCLUSION - PROSPECTS

Spectral energy distributions are a first useful and direct way to target first hydrostatic core candidates but high-resolution interferometry is definitely needed to determine the evolutionary stage of the observed sources. The capabilities of ALMA will enable us to make significant progress towards understanding the fragmentation at the early Class 0 stage and discovering first hydrostatic cores.

Our work is currently limited to the dust continuum emission, which cannot provide robust means yet to distinguish between FHSC and second hydrostatic cores and to decide on the nature of VeLLOs. Further work including molecular line emission calculations is thus warranted to better probe the physical conditions (density, temperature, etc.) in observed collapsing cores, for instance to disentangle the disk and the pseudo-disk, which should harbor different line profiles (rotation-dominated versus infall-dominated).

REFERENCES

[1] Commerçon, B., Launhardt, R., Dullemond, C. & Henning, Th. 2012, A&A, 545, 98
[2] Commerçon, B., Levrier, F., Maury, A.J., Launhardt, R., Henning, Th., 2012, A&A, 548, 39
[3] Teyssier, R. 2002, A&A, 385, 337
[4] Fromang, S., Hennebelle, P. & Teyssier, R. 2006, A&A, 457,371
[5] Teyssier, R., Fromang, S., Dormy, E., 2006, J. Comput. Phys., 218, 44
[6] Commerçon, B., Teyssier, R., Audit, E., Hennebelle, P. & Chabrier, G, 2011, A&A, 529, 35
[7] Semenov D., Henning, T., Helling, C., Ilgner, M. & Sedlmayr, E. 2003, A&A, 410, 611
[8] Commerçon, B., Hennebelle, P., Audit, E., Chabrier, G. & Teyssier, R. 2010, A&A, 510, L3
[9] Evans, II, N.J., Allen, L.E., Blake, G.A., et al., 2003, PASP, 115, 965
[10] Poglitsch, A., Waelkens, C., Geis, N., et al., 2010, A&A, 518, L2
[11] http://iram.fr/IRAMFR/GILDAS
[12] Pety, J., Gueth, F., Guilloteau, S., 2001, ALMA Memo 398